

## Evidence for Carbocation Intermediates in the TiO<sub>2</sub>-Catalyzed Photochemical Fluorination of Carboxylic Acids

Cuiwei Lai, Yeong Il Kim, Chong Mou Wang, and Thomas E. Mallouk\*

Department of Chemistry and Biochemistry, The University of Texas at Austin, Austin, Texas 78712

Received September 11, 1992

Laser flash photolysis/transient absorbance spectroscopy was used to determine the mechanism of photo-Kolbe fluorination of carboxylic acids, RCOOH → RF, at colloidal TiO<sub>2</sub> suspensions in acetonitrile. Transient absorption spectra of Ph<sub>3</sub>C<sup>+</sup>, Ph<sub>3</sub>C<sup>•</sup>, Ph<sub>2</sub>CH<sup>•</sup> and Ph<sub>2</sub>CH<sup>+</sup> were observed from the photooxidation of Ph<sub>3</sub>CCOOH and Ph<sub>2</sub>CCOOH at TiO<sub>2</sub> using 355-nm excitation. Transient decays, monitored in the presence and absence of fluoride ions, showed that the carbocations reacted rapidly with fluoride, but the neutral radicals did not. By varying the laser intensity, it was found that the photooxidation of Ph<sub>3</sub>CCOOH to Ph<sub>3</sub>C<sup>+</sup> at TiO<sub>2</sub> occurred via a single-photon process, while the formation of Ph<sub>3</sub>C<sup>+</sup> required two photons. This finding is in agreement with the parabolic light intensity dependence of initial reaction rates in bulk photolysis experiments. Although fluoride is strongly adsorbed on the TiO<sub>2</sub> surface in acetonitrile solution, the oxidizing power of photogenerated holes could be increased by coordinating HF to F<sup>-</sup>, and therefore the threshold for oxidative photochemical fluorination was extended to more positive potentials. In this way less easily oxidized carboxylic acids RCOOH could be converted to RF.

### Introduction

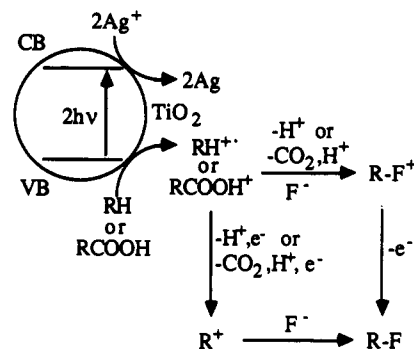
In the past few years, laser flash photolysis studies of colloidal TiO<sub>2</sub> suspensions have been used to determine the mechanism of photochemical reactions relevant both to solar energy conversion and to environmental remediation. These reactions have included reductions of methyl viologen<sup>1</sup> and H<sup>+</sup> (to form H<sub>2</sub>)<sup>2</sup> by conduction band electrons, and oxidation of halides,<sup>3</sup> OH<sup>-</sup> (to form O<sub>2</sub>)<sup>2</sup> and thiocyanate<sup>4</sup> with valence band holes. However, mechanistic studies of the reaction of valence band holes with organic substrates, which are relevant to semiconductor-catalyzed organic photoreactions, are very few.<sup>5</sup>

The photo-Kolbe reaction of carboxylic acids at illuminated TiO<sub>2</sub> surfaces, originally described by Kraeutler and Bard,<sup>6</sup> was one of the first useful semiconductor-catalyzed photoreactions to be reported. The predominance of radical coupling products in those reactions suggested that its mechanism resembles that of the electrochemical Kolbe reaction, in which reactive radicals are generated by one-electron oxidation and decarboxylation of RCOOH. Recently, we described a new, selective photochemical fluorination technique, in which organic substrates RH or RCOOH are converted to RF by an apparent two-electron oxidation,<sup>7</sup> according to reaction 1.



With this method, the organic substrate is oxidized at the

Scheme I. Two Possible Mechanisms for Photochemical Fluorination of RH and RCOOH with AgF/TiO<sub>2</sub>



surface of illuminated TiO<sub>2</sub> particles in the presence of AgF. Effectively, the excitation of the semiconductor with light of energy 3.0 eV or greater converts a weak oxidizer (Ag<sup>+</sup>) into a potent oxidizer (valence band hole), allowing an oxidative fluorination reaction to take place at the semiconductor surface. From bulk photolysis experiments it was argued that either neutral radicals or carbocations, generated by one- or two-electron oxidation of the organic substrate, respectively, were involved in the reaction. Two possible pathways, represented in Scheme I, were proposed: fluoride ion attack occurred either on the radical, and a second electron was subsequently transferred to the semiconductor to generate a monofluorinated product, or fluoride ions reacted only after two-electron oxidation of the substrate molecule. Bulk photolysis experiments reported previously could not eliminate either possible mechanism.

In this paper, we report nanosecond laser flash photolysis/transient absorbance experiments, carried out with colloidal TiO<sub>2</sub>, which establish that only the two-electron oxidation pathway is operative in the case of photo-Kolbe fluorination reactions. Using this mechanistic information, we have also been able to modify the conditions of the reaction (using HF to complex fluoride ions) in order to extend the method to less easily oxidized carboxylic acids.

(1) (a) Moser, J.; Gratzel, M. *J. Am. Chem. Soc.* 1983, 105, 6547. (b) Duonghong, D.; Ramsden, J.; Gratzel, M. *J. Am. Chem. Soc.* 1982, 104, 2977. (c) Bahnmann, D.; Henglein, A.; Spanhel, L. *J. Phys. Chem.* 1984, 88, 709.

(2) Duonghong, D.; Borgarello, E.; Gratzel, M. *J. Am. Chem. Soc.* 1981, 103, 4685.

(3) (a) Henglein, A. *Ber. Bunsenges. Phys. Chem.* 1982, 86, 241. (b) Moser, J.; Gratzel, M. *Helv. Chim. Acta* 1982, 65, 1436.

(4) Draper, R. B.; Fox, M. A. *J. Phys. Chem.* 1990, 94, 4628.

(5) Fox, M. A.; Lindig, B.; Chen, C. C. *J. Am. Chem. Soc.* 1982, 104, 5828.

(6) (a) Kraeutler, B.; Bard, A. J. *J. Am. Chem. Soc.* 1977, 99, 7729. (b) Kraeutler, B.; Bard, A. J. *J. Am. Chem. Soc.* 1978, 100, 2239. (c) Kraeutler, B.; Bard, A. J. *J. Am. Chem. Soc.* 1978, 100, 5985.

(7) Wang, C. M.; Mallouk, T. E. *J. Am. Chem. Soc.* 1990, 112, 2016.

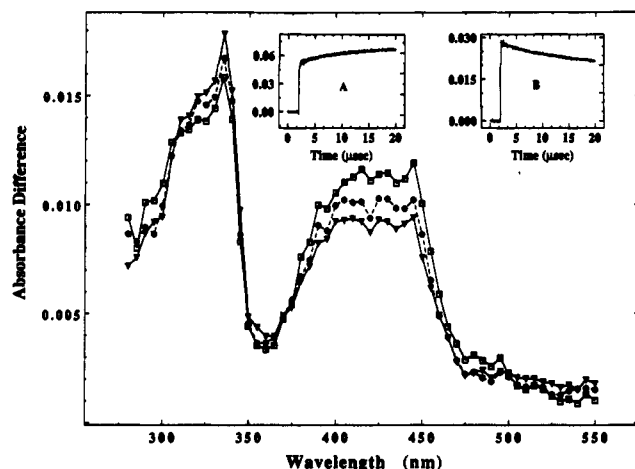


**Figure 1.** Transient absorption spectra generated by flash photolysis of colloidal  $\text{TiO}_2$  in 5 mM  $\text{Ph}_3\text{CCOOH}$  using 355-nm laser excitation ( $\square$ ) 5.9, ( $\bullet$ ) 29, and ( $\Delta$ ) 68  $\mu\text{s}$  after photolysis. Inset a: decay signal of  $\text{Ph}_3\text{C}^*$  at 335 nm. Inset b: decay signal of  $\text{Ph}_3\text{C}^+$  at 420 nm.

## Results and Discussion

**1. Transient Spectra of  $\text{Ph}_3\text{CCOOH}$  and  $\text{Ph}_2\text{CHCOOH}$  in  $\text{TiO}_2$  Suspensions.** Laser flash photolysis experiments were carried out in order to detect possible intermediates in the photo-Kolbe fluorination of carboxylic acids, according to reaction 1. Two substrates,  $\text{Ph}_3\text{CCOOH}$  and  $\text{Ph}_2\text{CHCOOH}$ , were chosen for this study because both are susceptible to photochemical fluorination with  $\text{TiO}_2/\text{AgF}$ , and because in both cases the proposed radical and carbocation intermediates can be easily identified from UV-visible spectra.

Figure 1 shows transient absorption spectra, taken several microseconds after 355-nm laser excitation of a deoxygenated, 5 mM colloidal  $\text{TiO}_2$  suspension in acetonitrile containing 5 mM  $\text{Ph}_3\text{CCOOH}$ . The suspension, prepared from a 2-propanol solution of titanium isopropoxide, was also approximately 100 mM in 2-propanol. The transient spectra show evidence for the essentially instantaneous formation of both one- and two-electron oxidation products, in comparable amounts. Spectra of  $\text{Ph}_3\text{C}^*$  and  $\text{Ph}_3\text{C}^+$  have been reported previously by Faria and Steenken,<sup>8</sup> who photolyzed an aqueous solution of  $\text{Ph}_3\text{CCOOH}$  using a 260-nm laser. In that work,  $\text{Ph}_3\text{CCOOH}$  was excited directly to form  $\text{Ph}_3\text{C}^*$  and then, after a second laser shot, ionized to form  $\text{Ph}_3\text{C}^+$ . The absorption spectra of the radical (335 nm) and cation (400–450 nm) are essentially identical to those shown in Figure 1. Further support for assignment of the 335-nm transient to  $\text{Ph}_3\text{C}^*$  comes from its rapid reaction with  $\text{O}_2$ , which acts as a radical scavenger. Peaks at 400–450 nm are attributed to the carbocation,  $\text{Ph}_3\text{C}^+$ . These peaks were unaffected by the presence of oxygen, but rapidly disappeared in the presence of fluoride ions (vide infra), presumably through reaction to form  $\text{Ph}_3\text{CF}$ . Control experiments showed that, in the absence of  $\text{TiO}_2$ , neither  $\text{Ph}_3\text{C}^*$  nor  $\text{Ph}_3\text{C}^+$  absorptions can be observed with 355-nm laser excitation, consistent with formation of these species by hole transfer from  $\text{TiO}_2$  rather than direct excitation.

From the insets a and b in Figure 1, it is apparent that the amount of  $\text{Ph}_3\text{C}^*$  grows with time following the laser flash, while the amount of  $\text{Ph}_3\text{C}^+$  decreases. Using the

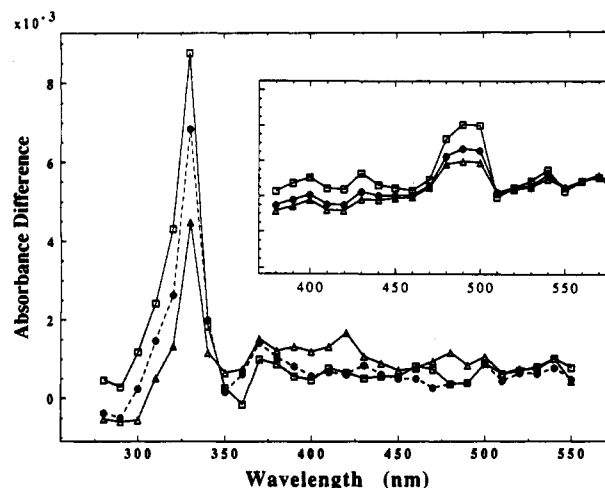


**Figure 2.** Transient absorption spectra of  $\text{Ph}_2\text{C}^*$  generated by flash photolysis of colloidal  $\text{TiO}_2$  in 5 mM  $\text{Ph}_2\text{CHCOOH}$  by 355-nm laser. ( $\square$ ) 5.7, ( $\bullet$ ) 29, and ( $\Delta$ ) 71  $\mu\text{s}$  after photolysis. Inset: transient spectra of  $\text{Ph}_2\text{C}^*$  generated under similar conditions, in the absence of 2-propanol.

extinction coefficients of  $\text{Ph}_3\text{C}^*$  ( $\epsilon = 3.6 \times 10^4 \text{ M}^{-1} \text{ cm}^{-1}$ )<sup>8</sup> and  $\text{Ph}_3\text{C}^+$  ( $\epsilon = 3.9 \times 10^4 \text{ M}^{-1} \text{ cm}^{-1}$ )<sup>9</sup> we calculate that the increase in  $\text{Ph}_3\text{C}^*$  concentration over 18  $\mu\text{s}$  is  $5.3 \times 10^{-8} \text{ M}$ , while the decrease in concentration of  $\text{Ph}_3\text{C}^+$  is  $5.8 \times 10^{-8} \text{ M}$ . The similarity of these decay traces suggests that  $\text{Ph}_3\text{C}^*$  is formed directly from  $\text{Ph}_3\text{C}^+$ , the most likely route being transfer of electrons trapped on  $\text{TiO}_2$  to the carbocation, since no electron scavenger is present in this experiment. Alternatively, it is possible that  $(\text{CH}_3)_2\text{COH}$  radicals generated from the hole scavenger, 2-propanol, reduce  $\text{Ph}_3\text{C}^+$  to form  $\text{Ph}_3\text{C}^*$ . At present we cannot differentiate the two possible sources of electrons for reduction of  $\text{Ph}_3\text{C}^+$ . In continuous photolysis experiments (vide infra), it is unlikely that either pathway for reduction of  $\text{Ph}_3\text{C}^+$  is very important, since an electron scavenger ( $\text{Ag}^+$ ) is used and no 2-propanol is present.

Figure 2 shows transient absorption spectra obtained under identical conditions, except that  $\text{Ph}_2\text{CHCOOH}$  was used in place of  $\text{Ph}_3\text{CCOOH}$ . The absorption transient at 330 nm was assigned to  $\text{Ph}_2\text{CH}^*$  since it is quenched rapidly by  $\text{O}_2$  but not by  $\text{F}^-$ . No visible transient, which might be attributed to the carbocation  $\text{Ph}_2\text{CH}^+$ , is seen here. This result is surprising, in light of the fact that  $\text{Ph}_2\text{CHCOOH}$  is converted to  $\text{Ph}_2\text{CHF}$  photochemically with  $\text{TiO}_2/\text{AgF}$  in ca. 30% yield.<sup>7</sup> We suggest that  $\text{Ph}_2\text{CH}^*$  is not oxidized to  $\text{Ph}_2\text{CH}^+$  under these conditions, because the 2-propanol present in the suspension is more easily oxidized by photogenerated holes at the  $\text{TiO}_2$  surface. When the solvent mixture (2-propanol and acetonitrile) of the colloidal  $\text{TiO}_2$  was removed in vacuo, a white powder was obtained and then redispersed in acetonitrile. A colloidal  $\text{TiO}_2$  suspension free of 2-propanol was then made by dispersing 5 mg of this powder in 4 mL of  $\text{CH}_3\text{CN}$ . Flash photolysis of this suspension, containing 5 mM  $\text{Ph}_2\text{CHCOOH}$ , gave a transient absorption peak at 480–490 nm (inset in Figure 2), which can be attributed to the carbocation  $\text{Ph}_2\text{CH}^+$ . The  $\text{Ph}_2\text{CH}^*$  and  $\text{Ph}_2\text{CH}^+$  peak maxima shown in Figure 2 correspond closely to the same

(8) Faria, J. L.; Steenken, S. *J. Am. Chem. Soc.* 1990, 112, 1277.

(9) McClelland, R. A.; Narinder, B.; Steenken, S. *J. Am. Chem. Soc.* 1986, 108, 7023.

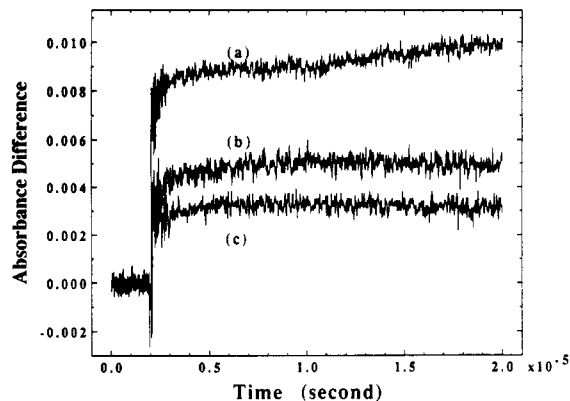


**Figure 3.** Decay of Ph<sub>3</sub>C<sup>•</sup> signal at 335 nm with (a) 0, (b) 1, (c) 2 mM tetraethylammonium fluoride (TEAF).

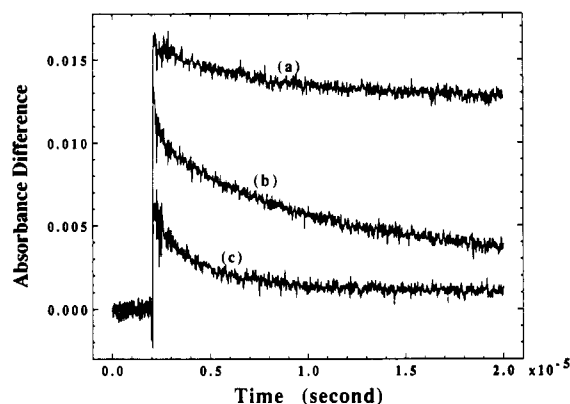


**Figure 4.** Decay of Ph<sub>3</sub>C<sup>+</sup> signal at 420 nm with (a) 0, (b) 1, (c) 2 mM TEAF.

species generated from Ph<sub>3</sub>CCl in acetonitrile solution by laser flash photolysis.<sup>10</sup>

Taken together, these transient spectra show that both radical and carbocation species are produced on a timescale of microseconds or less following UV laser excitation of TiO<sub>2</sub> colloids containing Ph<sub>3</sub>CCOOH or Ph<sub>2</sub>CHCOOH. Since the photogenerated radicals have minimal absorbance at the laser wavelength, 355 nm, and since a hole scavenger (2-propanol) suppresses the formation of the Ph<sub>2</sub>CH<sup>+</sup> carbocation, the most likely mechanism for formation of carbocations is transfer of two electrons per molecule to the semiconductor, rather than direct photoionization of radicals.

**2. Decay of Radical and Carbocation Signals in the Presence of F<sup>-</sup>.** The decay of photogenerated Ph<sub>3</sub>C<sup>•</sup> at different concentrations of F<sup>-</sup> is shown in Figure 3. On this timescale (20 μs) the radical is quite stable, being unreactive either with itself or with F<sup>-</sup>, as evidenced by the persistence of the transient signal. While it is clear that Ph<sub>3</sub>C<sup>•</sup> does not react rapidly with F<sup>-</sup>, the magnitude of the initial Ph<sub>3</sub>C<sup>•</sup> signal decreases significantly with increasing fluoride ion concentration. Figure 4 shows the decay of Ph<sub>3</sub>C<sup>+</sup> under similar conditions. Again, the height of the initial transient is decreased as fluoride is added to the suspension. An important difference in this case, however, is a significant increase in the decay rate of Ph<sub>3</sub>C<sup>+</sup> as more F<sup>-</sup> is added, consistent with a rapid reaction to form Ph<sub>3</sub>CF. The decay of Ph<sub>3</sub>C<sup>+</sup> does not follow simple

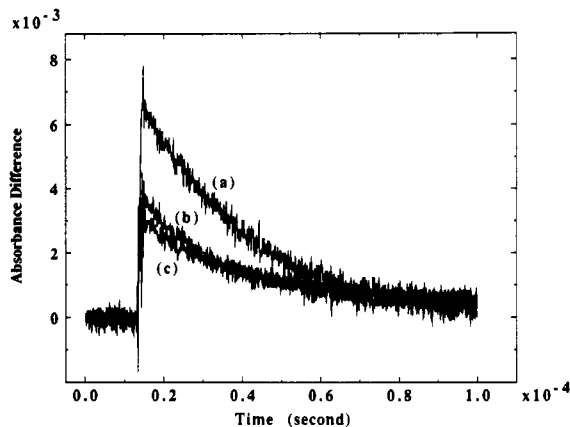


**Figure 5.** Decay of Ph<sub>2</sub>C<sup>•</sup> signal at 331 nm with (a) 0, (b) 1, (c) 2 mM TEAF.

second order kinetics because of strong adsorption of both F<sup>-</sup> and Ph<sub>3</sub>CCOOH at the TiO<sub>2</sub> surface (vide infra). Figure 5 shows the decay of photogenerated Ph<sub>2</sub>CH<sup>•</sup> at different concentrations of F<sup>-</sup>. As in the experiment with Ph<sub>3</sub>C<sup>•</sup> (Figure 3), the amount of radical initially produced decreases with increasing fluoride concentration, but the rate of decay of the Ph<sub>2</sub>CH<sup>•</sup> transient is independent of added fluoride, indicating that the radicals are unreactive with fluoride on this timescale.

The dependence of the amount of radicals (Ph<sub>3</sub>C<sup>•</sup> and Ph<sub>2</sub>CH<sup>•</sup>) produced initially on the fluoride concentration may be rationalized in terms of adsorption of fluoride ions at the semiconductor surface. Previous measurements of the TiO<sub>2</sub> flatband potential<sup>11</sup> have shown that fluoride strongly adsorbs onto the surface in acetonitrile solution, shifting the valence and conduction band edges to more negative potentials, as a consequence of the negative surface charge imparted by F<sup>-</sup>. Effectively, valence band holes photogenerated under these conditions are weaker oxidizers than those generated in the absence of strongly adsorbing anions. As more fluoride is added to the solution, the driving force for oxidation of Ph<sub>3</sub>CCOOH and Ph<sub>2</sub>CHCOOH becomes progressively weaker, the rate of electron transfer slows down, and therefore electron transfer from these molecules to TiO<sub>2</sub> competes less effectively with 2-propanol oxidation and electron-hole recombination.

**3. Light Intensity Dependence of Radical, Carbocation, and Product Formation.** Further support for the intermediacy of the carbocation Ph<sub>3</sub>C<sup>+</sup> in the production of Ph<sub>3</sub>CF from Ph<sub>3</sub>CCOOH comes from the light intensity dependence of both transients and products. Figure 6 shows that the transient absorbance corresponding to Ph<sub>3</sub>C<sup>•</sup> is linearly dependent on the intensity of the laser power, while the one for Ph<sub>3</sub>C<sup>+</sup> increases with the square of the laser power. We note that such power dependencies should be interpreted with caution, because of possible saturation effects at high laser power.<sup>12</sup> At the highest power used, a 15-ns laser flash delivers approximately 1 × 10<sup>17</sup> photons/cm<sup>2</sup> (with a 0.5 cm<sup>2</sup> spot size), and saturation effects are therefore expected for cases where the extinction coefficient of the absorber is ca. 3 × 10<sup>3</sup> M<sup>-1</sup> cm<sup>-1</sup>. For colloidal TiO<sub>2</sub> we estimate ε = 50 M<sup>-1</sup> cm<sup>-1</sup> at 355 nm; these experiments are therefore conducted

(10) (a) Bartl, J.; Steenken, S.; McClelland, R. A. *J. Am. Chem. Soc.* 1990, 112, 6918. (b) Bromberg, A.; Schmidt, K. H.; Meisel, D. *J. Am. Chem. Soc.* 1984, 106, 3056.

(11) Wang, C. M.; Mallouk, T. E. *J. Phys. Chem.* 1990, 94, 4276.

(12) Lachish, U.; Shafferman, A.; Stein, G. *J. Chem. Phys.* 1976, 64, 4205.

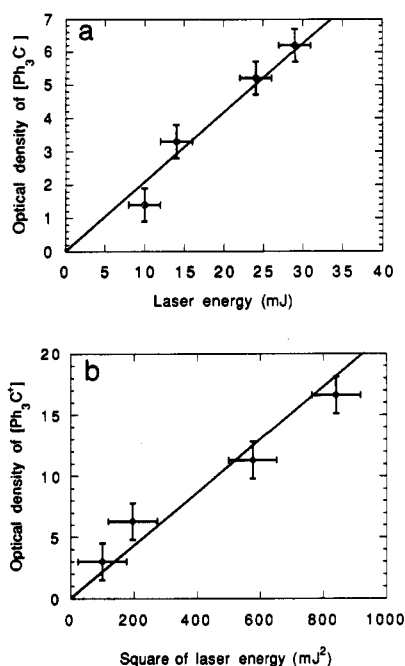


**Figure 6.** Plot of optical density of  $\text{Ph}_3\text{C}^+$  and  $\text{Ph}_3\text{C}^\cdot$  vs laser energy. The cation and radical were generated from solutions containing 5 mM  $\text{Ph}_3\text{CCOOH}$  and 5 mM colloidal  $\text{TiO}_2$  in acetonitrile. The laser energy was varied by means of screen filters.

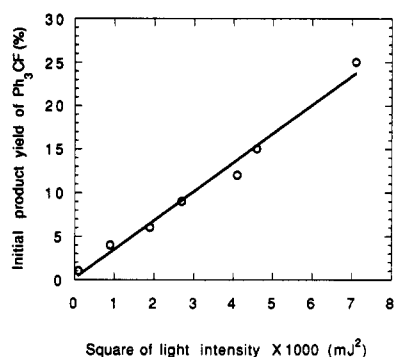


**Figure 7.** Initial rate of  $(\text{C}_6\text{H}_5)_3\text{CF}$  production vs light intensity. The reaction flask contained 50 mg of  $(\text{C}_6\text{H}_5)_3\text{CCOOH}$ , 50 mg of  $\text{AgF}$ , 10 mg of  $\text{KF}$ , 50 mg of  $\text{TiO}_2$ , and 2 mL of  $\text{CD}_3\text{CN}$ .  $\text{C}_6\text{F}_6$  was used as an external reference. Product yields were recorded after 1 h of illumination.

safely below the saturation threshold. Similar experiments were carried out for continuous photolysis of triphenylacetic acid in presence of  $\text{AgF}$ , using a Hg lamp attenuated by a 360-nm broad band filter. The initial reaction rate, taken as the  $^{19}\text{F}$  NMR yield of  $\text{Ph}_3\text{CF}$  after 1 h of continuous photolysis, was also found to vary with the square of the light intensity, as shown in Figure 7.

The linear and parabolic dependences of transient signal on laser power shown in Figure 6 imply that the production of  $\text{Ph}_3\text{C}^\cdot$  is a single-photon process, while the production of  $\text{Ph}_3\text{C}^+$  requires two photons. Consistent with the formation of  $\text{Ph}_3\text{CF}$  from  $\text{Ph}_3\text{C}^+$ , the light intensity dependence of reaction rate shown in Figure 7 is also that of a two-photon process.  $\text{Ph}_3\text{C}^+$  is produced by the reaction of  $\text{Ph}_3\text{C}^\cdot$  with  $\text{TiO}_2$  valence band holes, apparently before the latter can diffuse away from the surface of the semiconductor. Stepwise oxidation of  $\text{Ph}_3\text{C}^\cdot$  to  $\text{Ph}_3\text{C}^+$  is therefore not observed on the shortest observable timescale (ca. 100 ns) in the flash photolysis experiments.

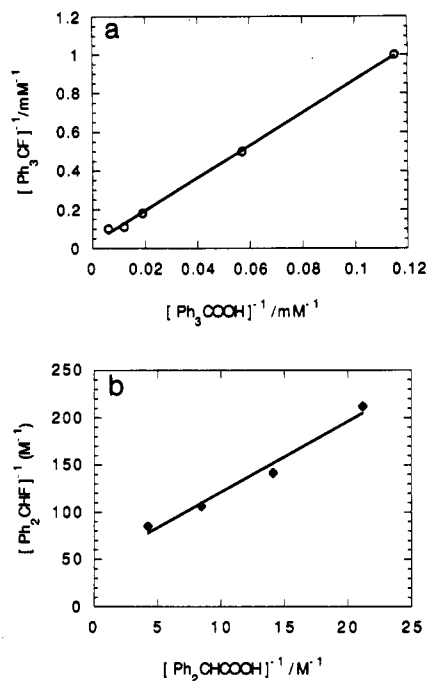


**Figure 8.** (a) Plot of reciprocal reaction rate vs reciprocal substrate concentration for  $\text{Ph}_3\text{CCOOH}$  fluorination. The reaction was run with  $\text{Ph}_3\text{CCOOH}$  amounts of 5–50 mg, 50 mg of  $\text{AgF}$ , 10 mg of  $\text{KF}$ , 50 mg of  $\text{TiO}_2$ , and 2 mL of  $\text{CH}_3\text{CN}$ . (b) Plot of reciprocal reaction rate vs reciprocal substrate concentration for  $\text{Ph}_2\text{CHCOOH}$  fluorination. Reaction conditions are the same as those used in part a.

**4. Langmuir–Hinshelwood Kinetic Analysis.** The Langmuir–Hinshelwood model can in many cases provide a quantitative kinetic treatment of solid–gas reactions. Recently a modified Langmuir–Hinshelwood treatment that includes solvent effects has been used to describe semiquantitatively the kinetics of solid–liquid reactions.<sup>13</sup> For the case of the photo-Kolbe fluorination reaction 1, if both  $\text{Ph}_3\text{CCOOH}$  and  $\text{F}^-$  are noncompetitively adsorbed at the surface of  $\text{TiO}_2$  and the concentration of  $\text{F}^-$  is held constant, then the reaction kinetics should be pseudo-first order. The rate ( $r$ ) of the reaction will be given by:

$$r = dC_A/dt = kK_A C_A / (1 + K_S C_S + K_A C_A) \quad (2)$$

$$r^{-1} = [(1 + K_S C_S) / kK_A] \cdot (1/C_A) + 1/k \quad (3)$$

Solvent effects are included in eqs 2 and 3, in which  $k$  is the reaction rate constant,  $K_A$  and  $K_S$  are Langmuir adsorption equilibrium constants for  $\text{Ph}_3\text{CCOOH}$  and solvent, and  $C_A$  and  $C_S$  are the concentrations of  $\text{Ph}_3\text{CCOOH}$  and solvent, respectively. Since the concentration of solvent is far greater than that of  $\text{Ph}_3\text{CCOOH}$  and remains essentially constant, the fractional coverage of the  $\text{TiO}_2$  surface by solvent can be assumed to be independent of the concentration of  $\text{Ph}_3\text{CCOOH}$ .

Figure 8, part a shows a plot of  $C_A^{-1}$  vs  $[\text{Ph}_3\text{CF}]^{-1}$ .  $[\text{Ph}_3\text{CF}]$  was recorded 30 min after the illumination and at this early stage of the photolysis is therefore proportional to the reaction rate. The plot is linear, indicating that the reaction involves adsorbed  $\text{Ph}_3\text{CCOOH}$ . This finding is

(13) (a) Al-Ekabi, H.; Serpone, N.; Pelizzetti, E.; Minero, C.; Fox, M. A.; Draper, R. B. *Langmuir* 1989, 5, 250. (b) Al-Ekabi, H.; Serpone, N. *J. Phys. Chem.* 1988, 92, 5726. (c) Al-Ekabi, H.; de Mayo, P. *J. Phys. Chem.* 1986, 90, 4075. (d) Hasegawa, T.; de Mayo, P. *Langmuir* 1986, 2, 362. (e) Al-Ekabi, H.; de Mayo, P. *Tetrahedron* 1986, 42, 6277.

Table I. Anodic Peak Potentials for Carboxylic Acids, Measured by Cyclic Voltammetry (scan rate 500 mV/s)

carboxylic acids	$E_p$ (V vs SCE)		products, yield <sup>a</sup> (%)	
			with AgF	with AgF·HF
Ph <sub>3</sub> CCOOH(1)		1.04	Ph <sub>3</sub> CF, 40	
Ph <sub>3</sub> COO-C <sub>8</sub> <sup>+</sup>		1.02 <sup>b</sup>		
Ph <sub>2</sub> C(CH <sub>3</sub> )COOH (2)	0.85	1.45	Ph <sub>2</sub> C(CH <sub>3</sub> )F, 30	
Ph <sub>3</sub> CCH <sub>2</sub> COOH (3)	0.66	1.46	Ph <sub>2</sub> CFCH <sub>2</sub> Ph, 60	
Ph <sub>2</sub> CHCOOH (4)	1.06	1.50	Ph <sub>2</sub> CHF, 30	
Ph <sub>2</sub> CHCOO-C <sub>8</sub> <sup>+</sup>		1.27 <sup>b</sup>		
PhC(CH <sub>3</sub> ) <sub>2</sub> COOH (5)	0.80	1.60	PhC(CH <sub>3</sub> ) <sub>2</sub> F, 10	PhC(CH <sub>3</sub> ) <sub>2</sub> F, 15
(CH <sub>3</sub> ) <sub>2</sub> CHCOOH (6)	0.70	1.85	(CH <sub>3</sub> ) <sub>2</sub> CH <sub>2</sub> , 20	(CH <sub>3</sub> ) <sub>2</sub> CHF, 15
(CH <sub>3</sub> ) <sub>2</sub> CHCOO-C <sub>8</sub> <sup>+</sup>	0.69	1.77 <sup>c</sup>		
(CH <sub>3</sub> ) <sub>3</sub> CCOOH (7)	0.70	2.00	(CH <sub>3</sub> ) <sub>3</sub> CH, 23	(CH <sub>3</sub> ) <sub>3</sub> CF, 10
(CH <sub>3</sub> ) <sub>3</sub> CCOO-C <sub>8</sub> <sup>+</sup>	0.94	1.83 <sup>c</sup>	(CH <sub>3</sub> ) <sub>3</sub> CO, 10	
PhCH <sub>2</sub> COOH (8)	0.60	2.20	PhCH <sub>2</sub> -CH <sub>2</sub> Ph, 90	PhCH <sub>2</sub> F, 5 <sup>d</sup>
PhCH <sub>2</sub> COO-C <sub>8</sub> <sup>+</sup>		1.43 <sup>b</sup>		

<sup>a</sup> Products were identified by <sup>19</sup>F NMR and mass spectral analyses. Yields reported are from integration of NMR spectra and do not represent isolated yields. <sup>b</sup> Reference 16. <sup>c</sup> Reference 17. <sup>d</sup> Yield by GC/MS analysis.

consistent with the proposed model of rapid two-electron oxidation of the organic substrate at the semiconductor surface, which competes with desorption of one-electron (radical) products. From the slope,  $(kK^{app})^{-1}$ , and intercept,  $k^{-1}$ , of the line in Figure 8, we calculate  $K^{app} = 0.003 \text{ M}^{-1}$  and  $k = 1.131 \text{ mM min}^{-1}$ , where  $K^{app} = K_A/(1 + K_S C_S)$ .

If we consider that both Ph<sub>3</sub>CCOOH and F<sup>-</sup> adsorb strongly on the semiconductor surface and may compete for the same sites, then the following form of the rate equations should be used:

$$\theta_A = (K_A C_A)/(1 + K_S C_S + K_A C_A + K_F C_F) \quad (4)$$

$$\theta_F = (K_F C_F)/(1 + K_S C_S + K_F C_F + K_A C_A) \quad (5)$$

$$\text{rate} = k\theta_A\theta_F =$$

$$kK_A C_A K_F C_F / (1 + K_S C_S + K_A C_A + K_F C_F)^2 \quad (6)$$

Here,  $\theta_A$  and  $\theta_F$  represent the fractional coverage of Ph<sub>3</sub>CCOOH and fluoride, respectively. However, eq 6 gives a substantially poorer fit to the data than eq 3. We tentatively conclude, therefore, that the noncompetitive adsorption model approximates the actual situation on the surface. Figure 8, part b shows a similar plot for the reaction of Ph<sub>2</sub>CHCOOH. Again, the linearity of the plot is consistent with noncompetitive adsorption of the carboxylic acid and fluoride ions at the TiO<sub>2</sub> surface.

**5. Tuning of the Flat Band Potential of TiO<sub>2</sub>.** Although fluoride is known to adsorb strongly at the TiO<sub>2</sub> surface, causing a negative shift in the semiconductor flat band potential (to -2.0 V vs SCE at monolayer coverage of F<sup>-</sup>, compared to -1.1 V in solutions of anions of lower charge density, such as ClO<sub>4</sub><sup>-</sup>), it is still possible to tune the flat band potential to more positive values by adjusting the ratio of HF to fluoride. Under these conditions, complex ions (HF)<sub>n</sub>F<sup>-</sup> are formed and adsorb strongly at the TiO<sub>2</sub> surface. Because of their lower charge density, these ions cause less of a negative shift than do uncomplexed fluoride ions, and indeed significant positive shifts are induced by dissociation of these ions to produce free HF.<sup>11</sup> In the present context, addition of HF to AgF/TiO<sub>2</sub> suspensions would be expected to increase the oxidizing power of valence-band holes, enabling one to prepare carbocation intermediates from less reactive carboxylic acids. At the same time, complexation of fluoride ions might be expected to reduce their reactivity with photogenerated carbocations. In order to determine the utility of flat band potential tuning in photo-Kolbe fluorination

reactions, we investigated the use of AgF·HF as the substitute for AgF. The bifluoride salt AgF·HF is easily prepared and handled, dissolves in acetonitrile without corrosion of contacting glassware, and is expected from previous measurements<sup>11</sup> to induce a positive flat band potential shift of ca. 0.7 V relative to AgF.

The first and second anodic peak potentials of several carboxylic acids were measured by cyclic voltammetry, and the results are compiled in Table I. In all cases, electrochemical oxidation was irreversible at the highest voltammetric scan rates used (1 V/s), and so anodic peak potentials, rather than formal potentials, were used to compare the relative ease of one- and two-electron oxidation of the various carboxylic acids. In TiO<sub>2</sub>/AgF/CH<sub>3</sub>CN suspensions, compounds 1-5, with second oxidation potentials less positive than 1.80 V vs SCE, can be photochemically fluorinated; however, compounds 6-8, with second oxidation potentials more positive than 1.80 V vs SCE, cannot. There is no apparent correlation between fluorination and the first oxidation potential, since compounds 6-8 are relatively easily oxidized by one electron. In these cases, GC/MS analyses revealed only radical coupling and oxygenation products, because no carbocations are generated photochemically. Under these conditions, photogenerated valence band holes are not sufficiently energetic to remove a second electron from compounds 6-8, in order to generate carbocations. We can conclude from these data that the oxidizing power of valence band holes lies between +1.6 and +1.8 V vs SCE in acetonitrile/AgF solutions.

By coordinating HF to F<sup>-</sup>, the threshold for oxidative photochemical fluorination is extended to the point where compounds 6-8 yield fluorinated products. The yields of these products are low, and products derived from radical intermediates still predominate. For example, in the case of phenylacetic acid (8), the fluorinated product PhCH<sub>2</sub>F is found in 5% yield, whereas a 50% yield of the radical coupling product PhCH<sub>2</sub>CH<sub>2</sub>Ph is obtained. Other radical coupling and oxygenation products, such as PhCHO, PhCHOH, and PhCH<sub>3</sub> are detected, in smaller amounts, by GC/MS analysis.

The fact that radical dimerization competes so effectively with fluorination suggests that in these cases desorption of the radical from the TiO<sub>2</sub> surface is kinetically very competitive with the second electron transfer step. Similar effects are apparent from the transient spectra shown for photoreactions of Ph<sub>3</sub>CCOOH and Ph<sub>2</sub>CHCOOH (Figures 1 and 2), in which both free radical

Table II.  $^{19}\text{F}$  NMR Chemical Shifts, Coupling Constants, and Mass Spectral  $m/z$  Values for Products of Photo-Kolbe Fluorination Reactions

compound	product <sup>a</sup>	$^{19}\text{F}$ NMR <sup>b</sup>	$m/z$
$\text{Ph}_3\text{CCOOH}$ (1)	$\text{Ph}_3\text{CF}$	-126.5 (s) <sup>c</sup>	262
$\text{Ph}_2\text{C}(\text{CH}_3)\text{COOH}$ (2)	$\text{Ph}_2\text{C}(\text{CH}_3)\text{F}$	-136 (q), <sup>d</sup> $J_{\text{HF}} = 21$ Hz	200
$\text{Ph}_3\text{CCH}_2\text{COOH}$ (3)	$\text{Ph}_2\text{CFCH}_2\text{Ph}$	-144.7 (t), <sup>d</sup> $J_{\text{HF}} = 48$ Hz	276
$\text{Ph}_2\text{CHCOOH}$ (4)	$\text{Ph}_2\text{CHF}$	-169 (d), <sup>d</sup> $J_{\text{HF}} = 48$ Hz	186
$\text{PhC}(\text{CH}_3)_2\text{COOH}$ (5)	$\text{PhC}(\text{CH}_3)_2\text{F}$	-135 (7), $J_{\text{HF}} = 21$ Hz	138
$(\text{CH}_3)_2\text{CHCOOH}$ (6)	$(\text{CH}(\beta)_2\text{CH}(\alpha)\text{F})$	-164 (7), <sup>e</sup> $J_{\text{H}(\alpha)\text{F}} = 50$ Hz, $J_{\text{H}(\beta)\text{F}} = 21$ Hz	62
$(\text{CH}_3)_3\text{CCOOH}$ (7)	$(\text{CH}_3)_3\text{CF}$	-132 (10), <sup>f</sup> $J_{\text{HF}} = 21$ Hz	76
$\text{PhCH}_2\text{COOH}$ (8)	$\text{PhCH}_2\text{CF}$	-210 (t), <sup>f</sup> $J_{\text{HF}} = 48$ Hz	110

<sup>a</sup> Products were identified by  $^{19}\text{F}$  NMR and mass spectral analyses. <sup>b</sup> Upfield from  $\text{CFCl}_3$ . <sup>c</sup> Reference 18. <sup>d</sup> Reference 7. <sup>e</sup> Reference 19. <sup>f</sup> Reference 20.

and carbocation intermediates are observed immediately following excitation. Indeed, in all these cases the low yields of fluorinated products can be attributed to competing radical reactions. In the case of  $\text{Ph}_2\text{CHCOOH}$ , for example,  $\text{Ph}_2\text{CHCOOH}$  is produced in 30% yield using  $\text{TiO}_2/\text{AgF}$ , along with radical coupling and oxygenation products,  $\text{Ph}_2\text{CHCHPh}_2$  (24%),  $\text{Ph}_2\text{CH}_2$  (14%),  $\text{Ph}_2\text{CO}$  (12%), and  $\text{Ph}_2\text{CHOH}$  (8%). Thus, while addition of HF to the reaction mixture effectively solves the problem of band energetics for all compounds studied, the problem of free radical reaction prior to the second electron transfer remains. For all compounds studied, the fluorination reaction is highly selective, with only one fluorinated product being observable in each case by  $^{19}\text{F}$  NMR.

### Conclusions

The laser flash photolysis studies reveal that carbocations, generated by two-electron oxidation of adsorbed substrate molecules, are intermediates of the photo-Kolbe fluorination of carboxylic acids in  $\text{TiO}_2/\text{AgF}$ /acetonitrile suspensions. In all cases free radical intermediates, which give rise to non-fluorinated radical coupling and oxygenation products, are also formed photochemically. The flat band potential of  $\text{TiO}_2$  can be tuned by adjusting the ratio of  $\text{HF}/\text{F}^-$  in the solution, and at a ratio of 1/1, photogenerated valence band holes are sufficiently oxidizing to produce fluorinated products (albeit in low yield) from a variety of aromatic and aliphatic carboxylic acids.

### Experimental Section

**1. Materials.** Titanium(IV) tetraisopropoxide (97%), diphenylacetic acid (99%), and triphenylacetic acid (99%) were obtained from Aldrich Chemical Co. and used as received. 2-Propanol (Mallinckrodt, analytical reagent), acetonitrile (Mallinckrodt, spectra grade), and anhydrous HF (Matheson) were also used without purification. Typically, acetonitrile and HF were handled on a stainless steel vacuum line and vacuum distilled at room temperature into the appropriate reactors.

Tetraethylammonium fluoride (Southwestern Analytical Laboratories) was prepared from the corresponding hydrate (Aldrich) by recrystallization/vacuum filtration five times from anhydrous diethyl ether/acetonitrile. The recrystallized salt was dried in vacuo overnight before use.

$\text{AgF}\cdot\text{HF}$  was made by vacuum transfer of excess HF onto solid  $\text{AgF}$  in a Teflon FEP tube, sealed at one end, on a stainless steel vacuum line. After mixing overnight, the  $\text{AgF}$  had dissolved in the HF completely. The excess HF was then pumped away through a soda-lime trap, and the salt was dried in vacuo over  $\text{P}_2\text{O}_5$  for 1 day. The ratio of HF to  $\text{AgF}$  was found to be  $1.0 \pm 0.15$  by titration with standard 0.1 N NaOH, using phenolphthalein as an indicator.

**2. Preparation of Catalysts.** For laser flash photolysis, acetonitrile suspensions of colloidal  $\text{TiO}_2$  were prepared by

hydrolysis of titanium tetraisopropoxide,<sup>5,14</sup> using procedures similar to those followed for aqueous colloids by Grätzel et al.<sup>2</sup> The water required for hydrolysis was provided in the concentrated perchloric acid used to acidify the colloid. Typically, 1 mL of  $\text{Ti}[\text{OCH}(\text{CH}_3)]_4$  was dissolved in 5 mL of 2-propanol. A volume of 0.85 mL of this solution was slowly injected (via microsyringe) into 100 mL of acidified acetonitrile (containing 0.3 M  $\text{HClO}_4$ ) with stirring. A transparent suspension of colloidal  $\text{TiO}_2$  was thus obtained with a  $\text{TiO}_2$  content of 5 mM. For the measurement involving  $\text{Ph}_2\text{CHCOOH}$  in an alcohol-free suspension, the solvents were vacuum-evaporated, leaving a dispersible white powder of  $\text{TiO}_2$ . The final transparent suspension was made by adding 5 mg of this powder to 4 mL of acetonitrile. Colloidal  $\text{TiO}_2$  suspensions prepared by either method were resistant to precipitation for at least 24 h and did not absorb in the visible region of the spectrum. For both colloids, an absorption band rose sharply in the UV at  $\lambda < 380$  nm. Fresh colloidal  $\text{TiO}_2$  suspensions were prepared before each set of experiments.

For continuous photolysis experiments, powdered rutile  $\text{TiO}_2$  was used. The powder was dried at 400 °C under vacuum overnight before use.

**3. Electrochemical Measurements.** Electrochemical measurements were carried out in a standard one compartment, three-electrode cell. The solution was acetonitrile containing 0.2 M tetrabutylammonium hexafluorophosphate as a supporting electrolyte and was 10 mM in the appropriate carboxylic acid. The working electrode was a platinum disk with a geometrical area of 0.2 cm<sup>2</sup>, and the reference electrode was a silver wire. A PAR Model 173/175 potentiostat/programmer (EG&G Princeton Applied Research, Princeton, NJ) was used to obtain i-V curves at scan rates of 500 mV/s. No correction for uncompensated resistance was made. The reference electrode was calibrated by addition of ferrocene,  $\text{Fe}(\text{C}_5\text{H}_5)_2$ , to the cell immediately following cyclic voltammetric measurements of substrate anodic peak potentials.

**4. Apparatus.** Flash photolysis experiments were carried out at the Center of Fast Kinetics Research at the University of Texas at Austin. A Quantel YG581 Nd:YAG Q-switched laser which produces 15-ns pulses at 355 nm was used. The diameter of the laser spot beam at the sample was ca. 0.8 cm. Beam energies of 10–28 mJ/pulse were typically found. The beam energy was reduced by means of screen filters. The laser shot energies were measured using a Scientech 370 energy meter. The experimental setup for transient absorbance measurements has been described in detail elsewhere.<sup>15</sup>

Continuous photolysis were carried out using a 500-W Hg lamp. The light beam was filtered by a 10-cm water jacket (to removed infrared radiation) and a 340-nm broad band filter. Light intensities were reduced by means of neutral density filters and were measured with a Coherent 210 power meter. The product yields for fluorination reaction were determined from integration of  $^{19}\text{F}$  NMR spectra. A Varian EM-390 spectrometer operating at 84.67 MHz was used to take  $^{19}\text{F}$  NMR spectra. Peak

(14) Kamat, P.; Fox, M. A. *Chem. Phys. Lett.* 1983, 102, 379.

(15) Persaud, L.; Bard, A. J.; Campion, A.; Fox, M. A.; Mallouk, T. E.; Webber, S. E.; White, J. M. *J. Am. Chem. Soc.* 1987, 109, 7309.

(16) Coleman, J. P.; Ebersson, L. *J. Chem. Soc., Chem. Commun.* 1971, 1300.

assignments were consistent with previous literature reports.<sup>7,17-19</sup> <sup>19</sup>F Chemical shift data and  $J_{\text{HF}}$  coupling constants for all compounds studied are given in Table II. EI/CI mass spectra were recorded on a Finnigan 4023 mass spectrometer.

---

(17) Reichenbacher, P. H.; Morris, M. D.; Skell, P. S. *J. Am. Chem. Soc.* **1968**, *90*, 3432.

(18) Williamson, S. M.; Gupta, D. D.; Shreeve, J. M. *Inorg. Synth.* **1986**, *24*, 66.

(19) Schmutzler, R. *J. Chem. Soc.* **1964**, 4551.

(20) Muller, N.; Carr, D. T. *J. Phys. Chem.* **1963**, *67*, 112.

The GC/MS spectra were recorded on a Varian 3400 gas chromatograph with a Finnigan Mat 700 ion trap detector. A SGE capillary column with a stationary phase of BPX 5, film thickness 0.5  $\mu\text{m}$  and 12-m length was used in GC analyses.

**Acknowledgment.** This work was supported by grants from the National Science Foundation (PYI Award CHE-8657729), the Texas Advanced Research Program, and the Welch Foundation. T.E.M. also thanks the Camille and Henry Dreyfus Foundation for support in the form of a Teacher-Scholar Award.